BMC Biotechnology

RESEARCH

Open Access

Chitosan-casein as novel drug delivery system for transferring Phyllanthus emblica to inhibit *Pseudomonas aeruginosa*

Helia Ramezani[1], Hossein Sazegar[1*] and Leila Rouhi[1]

Abstract

This study investigated the ability of *Phyllanthus emblica* encapsulated within chitosan-coated casein (CS-casein-Amla) nanoparticles to inhibit the growth of multi-drug-resistant *Pseudomonas aeruginosa* (*P. aeruginosa)* bacteria and prevent the formation of biofilms. The MDR strains underwent screening, and the morphological characteristics of the resulting nanoparticles were assessed using SEM, DLS, and FTIR. In addition, the efficacy of encapsulation, stability, and drug release were evaluated. The *PpgL*, *BdlA*, *and GacA* biofilm gene transcription quantities were quantified by quantitative real-time PCR. Simultaneously, the nanoparticles were assessed for their antibacterial and cytotoxic effects using the well diffusion and MTT procedures. CS-casein-Amla nanoparticles with a size of 500.73 ± 13 nm, encapsulation efficiency of 76.33 ± 0.81%, and stability for 60 days at 4 °C (Humidity 30%) were created. The biological analysis revealed that CS-casein-Amla nanoparticles exhibited strong antibacterial properties. This was shown by their capacity to markedly reduce the transcription of *PpgL*, *BdlA*, *and GacA* biofilm genes at a statistically significant value of $p \leq 0.01$. The nanoparticles demonstrated decreased antibiotic resistance compared to unbound Amla and CS-casein. Compared to Amla, CS-casein-Amla nanoparticles showed very little toxicity against HDF cells at dosages ranging from 1.56 to 100 µg/mL ($p \leq 0.01$). The results highlight the potential of CS-casein-Amla nanoparticles as a significant advancement in combating highly resistant *P. aeruginosa*. The powerful antibacterial properties of CS-casein-Amla nanoparticles against *P. aeruginosa* MDR strains, which are highly resistant pathogens of great concern, may catalyze the development of novel antibacterial research approaches.

Keywords *Pseudomonas aeruginosa*, Multi drug resistant, *Phyllanthus emblica*, Chitosan-casein, Antibiofilm

Introduction

In several areas worldwide, plants with therapeutic attributes have been used for millennia as conventional treatments for various human disorders [1]. Currently, there is a renewed interest in investigating safer biologically active compounds originating from natural sources that have an appropriate therapeutic index for the development of novel pharmaceuticals [2]. Phyllanthus emblica L., often referred to as Amla or Indian gooseberry, belongs to the Euphorbiaceae family and is routinely used in traditional medicine for its medicinal properties [3]. The constituents of P. emblica fruits mostly include tannins, polyphenolics, alkaloids, and other phytochemicals. The presence of tannins and polyphenols in P. emblica fruit suggests that vitamin C is very stable [4]. These phytochemicals increase antioxidant capability and efficiently neutralize free radicals. They also have anti-cancer, antibacterial, antifungal, antiviral, and anti-inflammatory

*Correspondence:
Hossein Sazegar
info.lactofeed1400@gmail.com; h.sazegar@iushk.ac.ir
[1]Department of Biology, Faculty of Basic Sciences, Shahrekord Branch, Islamic Azad University, Shahrekord, Iran

effects [5]. The increasing threat of antibiotic resistance in microorganisms has gotten severe in recent years. Microbial resistance is affected by several factors, one of which is biofilm [6].

Biofilms are complex structures formed by bacteria using proteins and external polysaccharides [7]. These biofilms are created by a variety of microorganisms working together in nature [6, 7]. *Pseudomonas aeruginosa* (*P. aeruginosa)* is a significant pathogen known for its capacity to produce biofilm and other bacteria [8]. *P. aeruginosa* infections are challenging to cure, mainly when they develop resistance to antibiotics and biofilm-forming agents [8, 9]. Hospital-acquired infections, particularly among individuals who are hospitalized for extended periods and have been exposed to invasive medical equipment, are prevalent [9]. Therefore, an effective and well-planned treatment plan is necessary [9, 10]. Moreover, the capacity of *P. aeruginosa* to create biofilms is a significant factor contributing to the ineffectiveness of treatments [10]. Biofilms protect bacteria against a range of environmental pressures, including UV radiation, drying out, lack of water, and antibacterial substances, ensuring their survival [11]. Bacteria may exhibit a significant decrease in antibiotic sensitivity, up to a thousand times, when they grow as a biofilm [10, 11]. The formation of biofilm and its subsequent removal may be complex due to several variables, including the surface qualities of the substrate, temperature, and oxygen levels [12]. Biofilms are more challenging to eradicate after they have taken hold on a surface, necessitating more forceful techniques [10–12]. Bacterial-resistant strains are becoming a significant problem due to the widespread and improper usage of antibiotics. Antibiotics' ability to eradicate germs has gotten less and less efficient. Higher dosages of antimicrobial agents are often needed to eradicate internal pathogens, which increases the risk of toxicity and adverse effects [13].

Biologically generated antibiofilm and antimicrobial compounds that are biodegradable, toxic-free, non-allergenic, economical, and ecologically beneficial became the subject of further research [14, 15]. Chitosan (CS), a biopolymer with numerous appealing reactive groups, has made it possible to produce drug carriers with varying physicochemical properties, including charge, hydrophobicity, and the dimension of particles [15]. CS has been used as a nanocarrier for several medications and vaccinations for oral, nasal, and ocular delivery routes [16]. Drug absorption was aided by the CS-based nanoparticles' regulated release and extended residence duration, especially for oral and intranasal administration [16, 17]. Additionally, these nano-systems demonstrated significant antibacterial and anti-biofilm properties to various microbes, such as Enterococcus faecalis and Listeria monocytogenes. The antibiofilm action of CS nanoparticles coated with antibiotics such as gentamicin versus L. monocytogenes biofilms was synergistic [18]. Furthermore, amikacin, vancomycin, and erythromycin formulations were effective versus L. monocytogenes [19], whereas oxacillin and chrysin CS-based compositions were successful versus Staphylococcus aureus [20]. In addition to delivering antibiotics, the function of CS-based nanoparticles also included the attachment of inorganic and organic chemicals from liquid solutions and the removal of other bacteria from water, such as S. aureus and *P. aeruginosa*. The grafted CS nanocomposite showed the efficient absorbance of lead ions (Pb+2) and the colorant methylene blue from the water. These results demonstrated the range of uses for CS nano-systems [21].

Chitosan nanoparticles have several applications, are crucial for drug administration, and exhibit antibacterial and antibiofilm properties; yet, due to their charge, these nano-systems face stability issues [22]. A positive charge is added to the nanoparticles using the cationic CS polymer [23]. As a result, these nanoparticles may significantly impact serum constituents. Also, these nanoparticles may aggregate and clear quickly, which would explain their poor activity [22, 23]. Casein surface alteration of CS nanoparticles is a straightforward and adaptable technique that may increase the stability of tiny CS nanoparticles [24]. Casein is built in moderate circumstances without heat or organic solvents [25]. Furthermore, by maintaining the integrity of the CS core, this change may result in an efficient carrier that can load medications like antibiotics efficiently. It is important to note that these systems show pH-dependent solubility, which may help with medication targeting [24, 25]. Numerous CS-coated microspheres, such as CS-alginate [11] and Cinnamaldehyde-coated chitosan, have been described as systems of antibiofilm and antibacterial action against multidrug-resistant microbial infections [26].

The study's main finding underscores the potential of polymer complexes, particularly those including chitosan, in enhancing efficiency. The pH of casein, which is 4.6, makes it an inadequate polyelectrolyte and protein. However, it becomes negatively charged at higher pH values [27]. In water conditions above the critical micellar concentration, casein can form micelles and demonstrate film-forming, clumping, and foaming capabilities. Its biodegradability, as demonstrated by its safe use in biomedical applications, make it a promising component [28]. Casein can interact with a variety of molecules and has both hydrophilic and hydrophobic regions [29]. Casein and chitosan are effective complexing/complex-forming partners due to their opposing charges at pH=6. The resulting structures can form balanced, water-soluble compounds or non-stoichiometric water-soluble combinations in excess of one of the complexation suppliers,

depending on the proportion among the functional groups inside the casein and chitosan structures [28, 29]. Casein is often used in medication delivery in the biomedical industry. Casein lacks reactive functional groups, which makes it regarded as chemically inert. Combining polycations and polyanions in solutions creates interpolymer compounds and casein independently (29, 30). The intermolecular forces for complexation are driven by the electrostatic contacts between oppositely charged microdomains of polyionic constituents. Other interactions, such as dipole interactions, hydrogen bonding, hydrophobic bonds, and van der Waals forces, aid the development of the complex. Casein coatings enhance the biomaterial's surface properties due to the interaction among polymers with opposing charges. Polymers' antibacterial activity may be modulated by casein [27–29].

The need for discovering and developing new, potent antimicrobial compounds is urgent. With the rise of multidrug-resistant *P. aeruginosa*, the availability of effective alternative antimicrobial medications is scarce. This underscores the critical importance of our research in the field of antimicrobial compounds and nanotechnology. This research aimed to examine the antibacterial and antibiofilm properties of *Phyllanthus emblica* encapsulated CS-casein nanoparticles on *P. aeruginosa*. *Phyllanthus emblica* encapsulated CS-casein nanoparticles' antibiofilm and antibacterial properties against various pathogenic *P. aeruginosa* were assessed. The synthesis of new biosynthesized *Phyllanthus emblica* encapsulated CS-casein nanoparticles is reported in this paper, along with an explanation of their morphological and structural properties and potential applications in medicine.

Materials and methods

Materials

Phyllanthus emblica (Amla) powder was purchased and phosphate buffer solution (PBS) from Merck (Germany). *Phyllanthus emblica* fruit was prepared in powdered form. Germany-based Merck provided the chitosan (1526.5 g/mol), casein, *tripolyphosphate (TPP*) and chloroform that were acquired. The following substances were purchased from Gibco, USA: Trypan blue, Medium RPMI-1640, Fetal Bovine Serum (FBS), and penicillin/streptomycin 100X. Sigma Aldrich (USA) provided the dialysis membrane with a molecular weight cut-off (MWCO) of 12,000 Da and MTT (dimethylthiazol-2-yl-)-2,5. We acquired H_2SO_4, Mueller Hinton Agar, and Mueller Hinton Broth from Merck in Germany.

Microbial analysis

Preparation of strains

P. aeruginosa ATCC 12,453 and 10 clinical *P. aeruginosa* strains were acquired from Parsian BioProducts Company. The bacteria strains were cultivated on Mueller Hinton agar (ZistYar Sanat Tech Dev Group, Iran) in oxygen at 37 ∘C for 24 h. One colony from each bacterial culture was transferred to Melluler-Hinton broth (ZistYar Sanat Tech Dev Group, Iran) and incubated at 37∘C. A similar amount was then taken from each broth to achieve an absorbance of 0.063 at 600 nm (10^8 CFU/mL), which was utilized for co-culture.

Testing for the sensitivity of bacteria to antibiotics

The disk diffusion technique was used to evaluate each bacterium's susceptibility to antibiotics according to the CLSI standard. Three to five colonies were chosen from pure culture and transferred into a tube containing 5 ml of sterile PBS. The solution was incrementally added while the temperature was consistently maintained at 37 °C until the suspension attained a density of 0.5 McFarland. The bacterial solution was applied to the sterile cotton swab, and the germs were spread evenly throughout the Mueller-Hinton agar. The plate surface was covered with antibiotic disks from MAST in England, which included imipenem (IMI, 10 µg), ceftazidime (CAZ, 30 µg), cefepime (FEP, 30 µg), ampicillin-sulbactam (SAM, 10 µg+10 µg), kanamycin (K, 30 µg), ciprofloxacin (CIP, 5 µg) and Colistin (COL, 10 µg). The diameter of the non-growth halo on the plates was measured following a 24-hour incubation period at 37 °C.

Biofilm formation assay

Congo red agar (CRA)

The CRA composition we developed included BHI at a concentration of 37 g/l, sucrose at 50 g/l, agar at 10 g/l, and a Congo red solution at 0.8 g/l. Subsequently, the bacterial strains were inoculated into plates containing the CRA media and incubated at 37 °C for 24 h. Under these circumstances, bacteria capable of constructing biofilms produce colonies that appear black, whereas other bacteria form red colonies [7, 11].

Microtiter plate assay (MPA)

In this research, 200 µl of the bacterium's culture was added to each well of a sterile 96-well polystyrene plate, and the bacteria were cultured for 24 h at 37ºC afterwards. A 200 µl volume of crystal violet dye with a concentration of 1% was used for staining. After 15 min, the dye was eliminated by rinsing it off with Phosphate-buffered saline (PBS). After adding 200 µl of acetic acid (33%), the optical density at 570 nm (OD570) was measured using the ELISA Reader Stat Fax2100 (Awareness Technology, Ukraine) [7, 11]. The bacteria that developed biofilms were categorized according to the data shown in Table 1.

Table 1 Classification of bacteria based on biofilm formation capacity

Biofilm Class	Results
OD > 4×ODc	Strong biofilm
2×ODc < OD ≤ 4×ODc	Medium biofilm
ODc < OD ≤ 2×ODc	Poor biofilm
OD ≤ ODc	Negative biofilm

Table 2 Sequence of primers used for real-time PCR

Name	5'----------->3'	Product Size	Tm (°C)	GenBank	Reference
16SrRNA	F: AAGCAACGCGAAGAACCTTA R: CACCGGCAGTCTCCTTAGAG	203 bp	58.0 °C	FJ972535.1	This study
GacA	F: CTGCGGTGAAGACTGTCTGA R: GACGGTGACTACCACGACCT	148 bp	58.0 °C	U27988.1	This study
BdlA	F: CAGATCACCTCGATCGTCAA R: GATCTCCTTGGTCGACTTGC	174 bp	58.0 °C	PP355094.1	This study
PpgL	F: GCACTCTGTTCGTGGTCAAC R: CTGGACCTGGCTGATCTGTT	119 bp	58.0 °C	OR855383.1	This study

Detection of *BdlA*, *PpgL* and *GacA* by PCR

The isolates were first introduced into LB agar and then incubated at 37 °C overnight. The DNA was obtained from isolated colonies using a genomic DNA extraction kit (ZistYar Salamat Tech Dev Group, Iran) following the directions provided by the manufacturer. This DNA was then utilized as the template for all amplifications. The genes associated with biofilm formation, namely *BdlA*, *PpgL*, and *GacA*, were amplified using standard PCR. Table 2 displays a compilation of primers, including their sequences, annealing temperatures, and the sizes of the amplified products used in this investigation [7, 11].

Nanobiotechnology analysis

Preparation of nanoparticles

The synthesis of Amla-coated CS-casein nanoparticles was conducted in a two-step process. Initially, CS-TPP-casein nanoparticles were synthesized using an ionic gelation technique that relies on the electrostatic attraction of the positively electrically charged chitosan and the negative-charged TPP. A suspension containing 0.01 mg/mL of CS in a 10% acetic acid solution with a concentration of 1% (w/v) was produced and allowed to sit on the magnetic stirrer for 24 h. Subsequently, the acidity level of the resulting solution was modified to 6.0 with the addition of sodium hydroxide. The chitosan (CS, 1526.5 g/mol) in the produced liquid was chemically bonded with 1% TPP (tripolyphosphate) by cross-linking. Next, the combination underwent centrifugation at a speed of 15,000 revolutions per minute at a temperature of 4 °C for 1.5 h. After that, it was mixed with casein utilizing an Ultrasonic mixer for 5 min. The Amla and CS-casein were merged in the second phase by magnetic attraction. A concentration of 10 mg/mL Amla and 5 mg/mL carbodiimide was added to the previously produced CS-casein particles to facilitate cross-linking with Amla. The solution was stirred overnight to ensure that the Amla coating adhered to the CS-casein via the development of an amide link between the carboxyl group of Amla and the amino group of the chitosan substrate. Ultimately, the pH was modified to fall between 4.2 and 6.5. Subsequently, the solution underwent ultracentrifugation for 1.5 h at a temperature of 4 °C. The resulting liquid above the sediment was removed, and the CS-casein-Amla nanoparticles were reconstituted in sterile water using ultrasonic processing. Free CS-casein was also used as a control group [7, 11].

Characterization of nanoparticles

Zeta potential (ZP) and median particle size (MPS) assessment

The ZetaPals instrument (Brookhaven Instruments Corp., USA) used palladium electrodes and dynamic light scattering machines to determine particle size and charge at 25 °C and a light scattering angle of 90°. The Nicomp® Nano ZLS System (Entegris, USA) was used to determine the MPS of the particles by laser diffraction. Water was used as the dispersant, and the refractive index was adjusted to 1.33. At a temperature of 25∘C, the nanosuspensions were diluted with distilled water. There were six assessments done in parallel [7, 11].

Field emission scanning electron microscopy (Fe-SEM)

The size of the nanoparticles was determined by analyzing field emission scanning electron microscopy (Fe-SEM) images. The morphology of the nanoparticles was examined using the field scanning electron microscopy (Fe-SEM) model MIRA3 (TESCAN, Czech Republic). Palladium was sputter-coated onto the samples to create a 5 nm thick layer, after which they were fixed to aluminum stubs using double-sided sticky adhesive disks made of conductive carbon (Quorum Q 150 R, Sussex, UK). The photos were taken at 10.00 kV [7, 11].

Attenuated total reflectance-fourier-transform infrared spectroscopy (ART-FTIR)

CS-casein-Amla nanoparticles were freeze-dried to assess the interaction between chitosan, Amla, and casein. Free-drying was used to obtain dry CS-casein-Amla nanoparticles using a Telstar, Lyo Alfa 15–85 plus type equipment (Telstar, Barcelona, Spain). The

nano-suspensions were frozen for 24 h at -80 °C in a deep freezer inside a round-bottom flask. Afterwards, the samples underwent a 24-hour freeze-drying process at 0.1 mbar to get a dry powder. The ART-FTIR (Brucker Alpha, USA) spectrometer was used to investigate powdered CS-casein-Amla nanoparticles in the 400–4000 cm-1 frequency range [7, 11].

Encapsulation efficiency

Following encapsulation, the efficacy of Amla's encapsulation (EE%) in CS-casein was evaluated. In conclusion, 1 mL of CS-casein-Amla nanoparticles was centrifuged for 1 h at 4 °C at a speed of 14,000 rpm. The maximum adsorption of the precipitate at an emission wavelength of 653 nm was used to calculate the encapsulated Amla content in each sample [7, 11]. Next, the percentage of the encapsulation efficacy was calculated using the following formula:

EE%= Total amount of initial Amla entrapped into the CS-casein formulations – the amount of free Amla in supernatant/ total amount of drug × 100.

Preparation of solution

Initially, 100 mg of amla, CS-Casein and CS-amela powder was dissolved in 1000 ml of distilled water. Subsequently, serial dilution was performed three times until the solution concentration reached 100 µg/mL. This solution was applied in experiments.

In vitro stability and drug release study

The medicine was discharged in a lab using a dialysis bag with a molecular weight cut-off (MWCO) of 12 kDa. To do this, 2 mL of Amla and 2 mL of CS-casein-Amla nanoparticles were added to the dialysis bag. The whole combination was then submerged in a 50 mL PBS solution with a pH of 7.4. At 37 °C and 50 rpm, the resultant solution was gently mixed. It was then separated into equal halves at regular intervals, and a new environment was added. Moreover, an identical procedure was performed for the unbound Amla. Throughout a two-month storage period, measurements were taken at 0, 15, 30, 45, and 60 days at 4 and 25 °C [7, 11].

Antibacterial analysis of nanoparticles

Broth microdilution assay

The broth microdilution method determined the minimum inhibitory concentration (MIC). To summarize, several concentrations of CS-casein, Amla, and CS-casein-Amla, which varied from 0.781 to 100 µg/mL, were added to the 96-well plate. Afterwards, 100 µL of the microbial solution was added to each well, and the plates were incubated overnight at 37 °C. The turbidity of all wells was measured using the ELISA Reader Stat Fax2100 (Awareness Technology, Ukraine) equipment at a wavelength of 630 nm. Two wells were selected as the negative control, consisting only of culture media, and the positive control, consisting of culture medium with *P. aeruginosa* ATCC 12,453. The minimum inhibitory concentration (MIC) values, the lowest levels of medicine that prevent bacterial growth, and the sub-MIC levels, the highest levels of pharmaceuticals that do not affect bacterial growth, were determined [7, 11].

Agar Well Diffusion assay

The antimicrobial activity of CS-casein, Amla, and CS-casein-Amla was evaluated using the agar well diffusion technique on Mueller Hinton Agar (MHA) plates. The *P. aeruginosa* strains were introduced into the Nutrient broth and allowed to grow overnight at a temperature of 37 °C until the turbidity reached a level equivalent to 0.5 McFarland standards, resulting in a final inoculum concentration of 1.5×10^8 CFU/ml. Using a sterile cork-borer (6 mm), 4 wells measuring 6 mm were bored into the inoculation medium. Each well was filled with 50 µl of CS-casein, Amla, and CS-casein-Amla and negative/solvent control (PBS). The solution was let to disperse for about 30 min at ambient temperature and then placed in an incubator for 18–24 h at 37 °C. Following incubation, the plates were examined for a distinct area devoid of growth surrounding the well, indicating the antimicrobial effectiveness of the investigated substances. The ruler was used to measure areas where bacterial growth was inhibited. The area of bacterial growth inhibition, known as the zone of inhibition (ZOI), was visually inspected and quantified in millimeters (mm) [7, 11].

Time kill assay

The time-kill experiment included subjecting bacteria to CS-casein, Amla, and CS-casein-Amla at concentrations below the minimum inhibitory concentration (MIC). To summarize, the bacterial growth study included testing the effects of CS-casein, Amla, and CS-casein-Amla at concentrations below the minimum inhibitory concentration (sub-MIC) on each bacterium being studied. To summarize, 100 µL of each specimen was mixed with 100 µL of each bacteria solution, resulting in a final concentration of 10^5 CFU/mL for each bacterium. The specimens were subjected to a controlled environment with a temperature of 37 °C, and the light absorption was monitored at different time intervals over 24 h (0, 4, 8, 12, 16, 20, 24) [7, 11].

Analysis of Biofilm Growth Inhibition percentage (BGI%)

The efficacy of CS-casein-Amla nanoparticles in inhibiting biofilm formation by adhering to model biofilms was assessed by quantifying the decrease in OD630 of biofilms after a 24-hour exposure to free CS-casein and Amla. The wells harboring biofilm were exposed to

200 µl of CS-casein-Amla solution at different concentrations (1/2MIC, MIC and 2 MIC). CS-casein and Amla served as control samples. Following a 24-hour incubation period at a temperature of 37 °C, the liquid components of each well were removed, and the biofilms were cleansed using ethanol. Subsequently, a culture without antibiotics was introduced into the wells, and the liquid portion of the biofilm and aspirate were then treated with a fixing agent and rinsed. The biofilms were then dyed with violet crystal, and their light absorbance was quantified using the LISA Reader Stat Fax2100 (Awareness Technology, Ukraine) at a wavelength of 630 λmax nm [7, 11]. The degree of inhibition of biofilm development (%BGI) was calculated using the following equation:

Biofilm gene expression analysis

The effect of CS-casein, Amla, and CS-casein-Amla on the transcription of *PpgL*, *BdlA*, *and GacA* biofilm genes in *P. aeruginosa* strain was assessed utilizing quantitative Real-Time PCR. The whole RNA extraction was done using a total RNX-Plus kit (Cinnagen Co., Iran) on samples treated with sub-MIC quantities of CS-casein, Amla, and CS-casein-Amla. The cDNA was synthesized utilizing the YTA Kit Protocol given by Yekta Tajhiz, an Iranian business. A real-time polymerase chain reaction (PCR) assay was performed utilizing the YTA SYBR Green master mix manufactured by Yekta Tajhiz, in Iran. The 16SrRNA gene was used as an internal control, as shown in Table 2. For Real Time-PCR, a reaction consisting of 15 µL was produced. The volume consisted of 0.5 µL of cDNA, 0.5 µL of forward primer, 0.5 µL of reverse primer, 10 µL of master mix, and 3.5 µL of double sterile distilled water. The temperature-dependent cycle program included an initial denaturation stage at 95 °C for 10 min, followed by 40 cycles at 95 °C for 30 s and 58 °C for 40 s. The primer sequences for the target genes, namely *PpgL*, *BdlA*, *GacA*, and 16 S rRNA (used as an internal control), can be found in Table 2 [7, 11].

Cytotoxicity assay

The MTT colorimetric examination, carried out by Kalazist in Iran, evaluated the cytotoxicity of CS-casein, Amla, and CS-casein-Amla. 20,000 healthy human dermal fibroblast (HDF) cells were cultured in 96-well plates utilizing RPMI1640 media enriched with 10% fetal bovine serum. After that, the plates were placed in a CO2 incubator and incubated at a temperature of 37∘C. The cells were subjected to CS-casein, Amla, and CS-casein-Amla at concentrations ranging from 1.56 to 100 µg/mL. After incubation, 20 µL of the MTT solution (5 mg/mL) in the PBS (Kalazist, Iran) was added to each well. After 4 h of incubation, the liquid in the container was removed, and 100 mL of DMSO was added to the 96-well plates. The plates were agitated at a speed of 400 rpm for 6 min to dissolve the formazan crystals that had grown in DMSO completely. The color intensity was measured utilizing an ELISA Reader Stat Fax2100 (Awareness Technology, Ukraine) at a wavelength of 570 nm. The cell viability was quantified as the average ± standard deviation (SD) ($n=5$). As a control, HDF cells were grown using RPMI1640 media that did not include the test sample [7, 11]. The proportion of viable cells was calculated using the following equation:

Statistical analysis

The statistical analysis in this study was conducted using SPSS software version 20, and the resulting data was evaluated utilizing one-way analysis of variance (ANOVA). The transcription levels of target genes in both the control and treatment samples were assessed using Tukey's HSD post-statistical approach.

Results

Microbial analysis results

Antibiotic susceptibility profile

This study included the acquisition of 10 strains of *P. aeruginosa*, which were procured and identified by ZistYar Salamat Tech Dev Group in Tehran, Iran. The antibiotic susceptibility testing shows that imipenem had the most significant resistance (100%, 10 strains) among the 8 selected antimicrobial agents. Kanamycin followed with a resistance rate of 90% (9 strains), ceftazidime with 70% (7 strains), ampicillin-sulbactam with 60% (6 strains), piperacillin-tazobactam with 50% (5 strains), Colistin with 40% (4 strains), cefepime with 30% (3 strains), and the slightest resistance was detected with ciprofloxacin at 30% (3 strains). Multidrug-resistant (MDR) isolates were defined as those that exhibited resistance to three or more antibiotic classes based on the data shown in Table 3.

Biofilm formation assay

Among the 10 MDR strains, 10 strains (100%) showed the development of rough black colonies, while the remaining 0 strains (0%) were classified as non-producers with smooth white colonies. The microtiter plate findings showed that of the 10 strains examined, 8 strains (80%) were categorized as strong biofilm producers, while 2 strains (20%) were categorized as moderate biofilm providers (Table 4).

PCR amplification of *GacA*, *BdlA* and *PpgL* gene

Table 4 illustrates the *GacA*, *BdlA*, and *PpgL* gene amplification using polymerase chain reaction (PCR). In addition, all 10 biofilm-positive strains of *P. aeruginosa* capable of developing resistance to several drugs were shown to possess the *GacA*, *BdlA*, and *PpgL* genes. PCR amplification of genes yielded amplicons of different

Table 3 Antibiotic resistance pattern to *P. Aeruginosa*

Class	Symbol	Antimicrobial Agent	Disk content (µg)	Susceptible (S)	Intermediate(I)	Resistant(*R*)	Number of resistant strains	Percentage of resistant strains	Total
Carbapenems	IMI	Imipenem	10 µg	≥ 22	19–21	18 ≥	10	100%	10 Strain
Ureidopenicillins	PTZ	Piperacillin-tazobactam	100/10µg	≥ 21	18–20	17 ≥	5	50%	
Sulfonamide + inhibitor	SAM	Ampicillin-sulbactam	10 µg + 10 µg	≥ 15	12–14	11 ≥	6	60%	
Aminoglycosides	K	Kanamycin	30 µg	≥ 17	15–16	14≥	9	90%	
Cephalosporins	CAZ	Ceftazidime	30 µg	≥ 18	15–17	14 ≥	7	70%	
	FEP	Cefepime	30 µg	≥ 18	15–17	14 ≥	3	30%	
Colistin	COL	Colistin	10 µg	2≥	-	≥ 4	4	40%	
Quinolones	CIP	Ciprofloxacin	5 µg	≥ 17	15–16	14≥	3	30%	

Table 4 Biofilm formation results in isolated MDR *P. Aeruginosa*

Isolated bacteria	Biofilm formation ability				Biofilm gene			MDR
	CRA test	MPA TEST						
		OD_C	OD	Biofilm Class	GacA	BdlA	PpgL	
Strain 1(S1)	+	0.082	0.352	Strong	+	+	+	+
Strain 2(S2)	+	0.072	0.134	Strong	+	+	+	+
Strain 3(S3)	+	0.009	0.026	Medium	+	+	+	+
Strain 4(S4)	+	0.013	0.153	Strong	+	+	+	+
Strain 5(S5)	+	0.014	0.111	Strong	+	+	+	+
Strain 6(S6)	+	0.009	0.032	Medium	+	+	+	+
Strain 7(S7)	+	0.011	0.131	Strong	+	+	+	+
Strain 8(S8)	+	0.062	0.248	Strong	+	+	+	+
Strain 9(S9)	+	0.015	0.109	Strong	+	+	+	+
Strain 10(S10)	+	0.009	0.116	Strong	+	+	+	+

sizes: 148 base pairs for the *GacA* gene, 174 base pairs for the *BdlA* gene, and 119 base pairs for the *PpgL* gene (Fig. 1A).

Nanobiotechnology analysis results

Size and ZP measurements of the nanoparticles

The MPS of the CS-casein and CS-casein-Amla particles were 425±0.14 nm and 698±0.57 nm, respectively. The results acquired from the FeSEM images indicated that the CS-casein and CS-casein-Amla had an average size of 402.25±22 nm and 500.73±13 nm, respectively. The scanning electron microscopy (FeSEM) image of CS-casein and CS-casein-Amla nanoparticles (Fig. 1B) demonstrates the existence of approximately spherical particles evenly dispersed within the nanometer scale. Furthermore, Fig. 1C displays the particle size distribution analysis outcomes for CS-casein and CS-casein-Amla nanoparticles. The CS-casein and CS-casein-Amla exhibited Zeta Potential (ZP) values of -41.3±2.88 and −35.7±3.41 millivolts (mV) respectively (Fig. 2A). Considering that chitosan has a positive charge, the presence of a negative charge in CS-casein and CS-casein-Amla compounds indicates the negative charge of casein. Table 5 also displays the morphological features of the CS-casein and CS-casein-Amla nanoparticles.

Fourier transform infra-red (FT-IR) analysis

Figure 2B displays an FTIR spectrum of Amla, CS-casein and CS-casein-Amla nanoparticles. The CS-casein exhibited distinct peaks at 3264.73, 1453.82 cm^{-1} corresponding to O–H and 874.49, 1594.78 cm^{-1} corresponding to C=O (amide). The peaks seen at 2944.84 and 1044.58 cm^{-1} were identified as the result of C–H and C-O bond stretching in CS-casein, respectively. Amla exhibited distinct peaks at 2944.84, 1453.82 cm^{-1} corresponding to O–H and at 433.57, 601.61, 730.74, 877.19, 1664.78 cm^{-1} corresponding to C=O (amide). The peaks seen at 1084.83 and 1044.58 cm^{-1} were identified as corresponding to the stretching of C–H and C-O bonds in CS-casein, respectively.

The absorbance peaks at 2980.79, 2424.84, and 1628 cm^{-1} were observed for CS-casein-Amla nanoparticles, which may be attributed to the absorption of –NH3+in CS-casein. Another distinct peak was seen at 1084.83 cm^{-1}, providing compelling evidence of the existence of NH3+in CS-casein-Amla nanoparticles. Furthermore, the other peaks seen in CS-casein-Amla were comparable to those found in Amla. The peak seen at 2924.88 cm^{-1} corresponds to the stretching vibrations of –OH and –NH groups, as well as intermolecular hydrogen bonding, reinforcing our understanding of the nanoparticles.

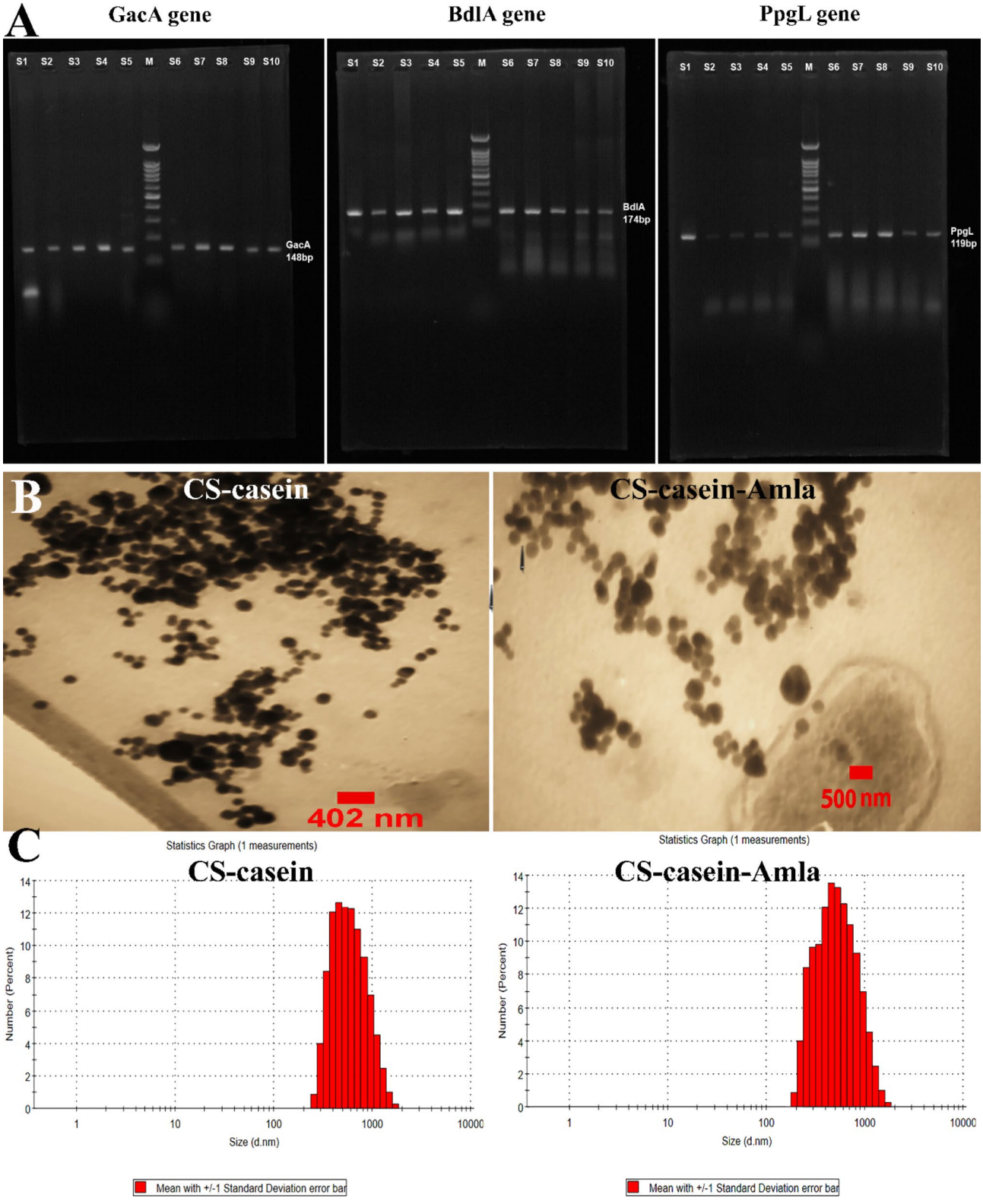

Fig. 1 **A**) *GacA*, *BdlA*, and *PpgL* gene amplification using polymerase chain reaction (PCR). **B**) The appearance and size of produced CS-casein and CS-casein-Amla nanoparticles were measured using Field Emission Scanning Electron Microscopy (FeSEM). **C**) Quantifying the size dispersion of CS-casein and CS-casein-Amla nanoparticles by DLS analysis

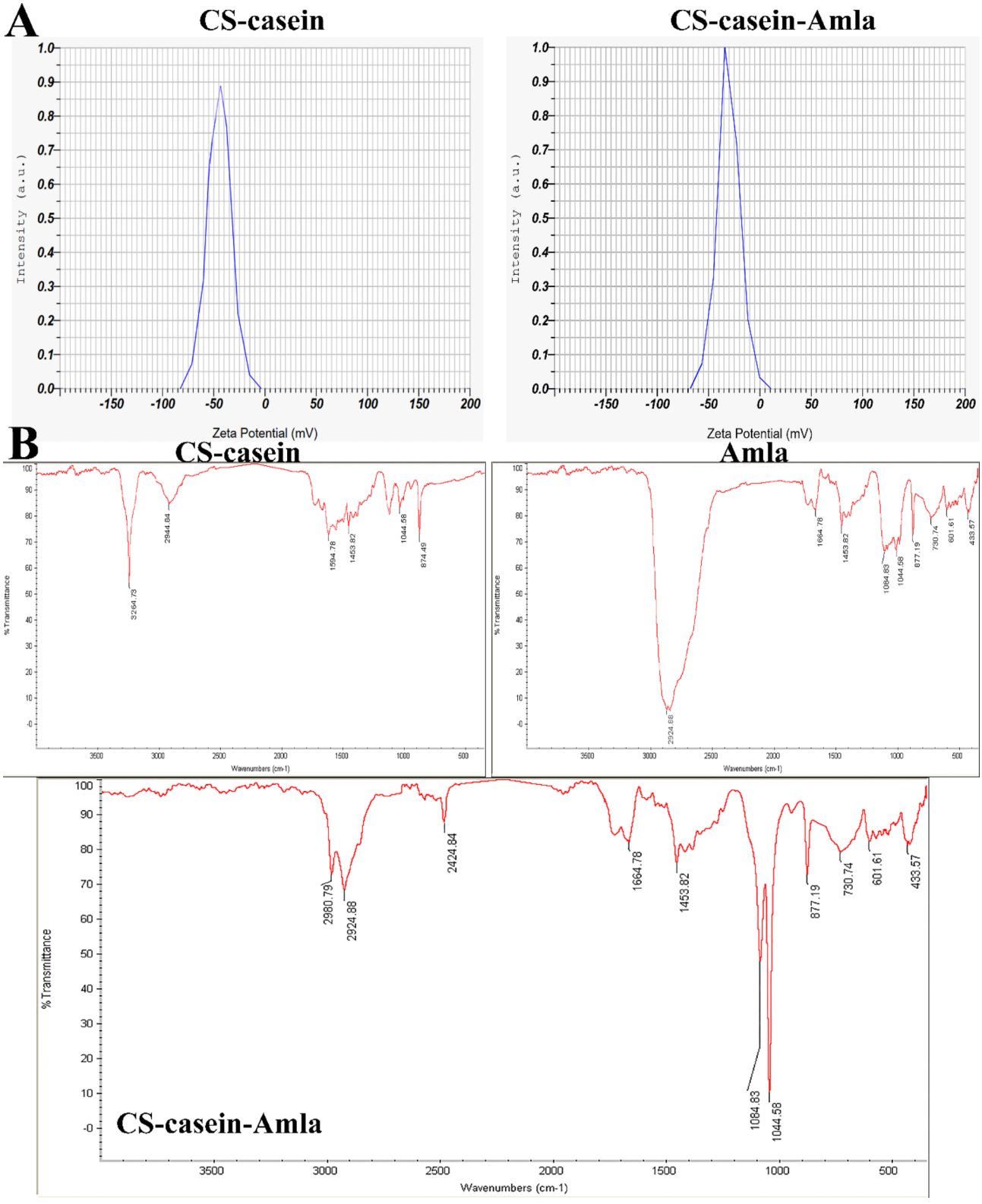

Fig. 2 (**A**) The zeta potential values for CS-casein and CS-casein-Amla nanoparticles were −41.3 ± 2.88 and −35.7 ± 3.41, respectively. (**B**) Fourier Transform Infrared (FTIR) spectra of Amla, CS-casein and CS-casein-Amla nanoparticles

Table 5 Characterization of synthesized nanoparticles. Data are represented as mean ± SD, $n = 3$

Nanomaterials	Polydispersity index (PDI)	Surface charge (mv)	FeSEM (nm)	DLS (nm)	EE (%)
CS-casein	0.46 ± 0.043	-41.3 ± 2.88	402.25 ± 22	425 ± 0.14	---
CS-casein-Amla	0.31 ± 0.074	-35.7 ± 3.41	500.73 ± 13	698 ± 0.57	76.33 ± 0.81

Encapsulation efficiency and in-vitro drug release

This study aimed to examine the influence of CS-casein on the entrapment of Amla and its subsequent release actions. CS-casein-Amla nanoparticles' encapsulation effectiveness (EE%) was determined to be 76.33±0.81, as shown in Table 5.

Figure 3A depicts the emission profile of Amla from the dialysis tube that holds the Amla solution and CS-casein-Amla nanoparticles. Figure 3A illustrates that including Amla in CS-casein successfully inhibits sudden and rapid release. The release profile exhibited an early period of fast release extending up to 6 h, accompanied by a following phase of slower release reaching up to 120 h. Based on the data in Fig. 3A, the percentage of free Amla released during the first 6-hour period is 84%. Subsequently, the release maintains a high level of consistency, with the whole amount of Amla being released within 72 h. The proportion of drug released in the CS-casein-Amla nanoparticles is 57% during 72 h, and it subsequently jumps to 97% after 120 h.

Physical stability study of nanoparticles

The dimensional stability of CS-casein and CS-casein-Amla nanoparticles was assessed by measuring the size of the encapsulated nanoparticles and the percentage of medicine remaining after preservation at refrigerator (4±2 °C) and room temperatures (25±2 °C). The motions were slower at 4±2 °C than at 25±2 °C, as can be seen by looking at the difference in mean diameter. The drug preservation in CS-casein-Amla nanoparticles exhibits a drug leakage rate of less than 20% from the initial quantity in both circumstances, as shown in Fig. 3B. The results indicate that the CS-casein-Amla nanoparticles have strong physical stability and might be used effectively to prevent medicine leakage. According to the results demonstrated by Fig. 3B, the dimension of the Free CS-casein grows in proportion to the amount of time it is stored ($P<0.01$). The sample maintained at a temperature of 4±2 °C demonstrates higher stability in comparison to the sample kept at a temperature of 25±2 °C (Fig. 3C). The enhanced stiffness of the hydrophobic portion of CS-casein at lower temperatures might explain this phenomenon [49].

Antibacterial tests

Determination of MIC and sub-MIC

The microbicidal and sub-microbicidal effects of Amla, CS-casein, and CS-casein-Amla against biofilm-forming *P. aeruginosa* were investigated using a microtiter plate. The Amla MIC determinations indicated that all strains of *P. aeruginosa* had MIC values ranging from 25 to 50 µg/mL, as shown in Table 6. The investigation of the CS-casein-Amla nanoparticles MIC revealed that all isolates of *P. aeruginosa* had MIC concentrations ranging from 1.56 to 3.125 µg/mL (Table 6). Table 6 shows that CS-casein-Amla nanoparticles' minimum bactericidal concentration (MBC) values were consistently twice as high as the MIC amounts. However, the CS-casein-Amla nanoparticles demonstrated MIC and MBC levels versus the tested strains of bacteria that were double the values of free Amla. Table 6 shows that the MIC of free CS-casein versus *P. aeruginosa* was 50 µg/mL.

Nevertheless, strain 1, strain 7, and strain 10 did not show any MIC while exposed to free CS-casein. However, no growth inhibition was seen with CS-casein-Amla nanoparticle concentrations of 3.125 µg/mL. The highest sub-MIC level for CS-casein-Amla nanoparticles was 0.781 µg/mL. The studies used this concentration to inhibit biofilm development (MBIC). Moreover, the MIC was significantly reduced—by two to four times—when CS-casein-Amla nanoparticles were used instead of free CS-casein and free Amla. These findings demonstrate that the CS-casein-Amla nanoparticles significantly enhanced Amla's antibacterial efficacy.

Antimicrobial activity of nanoparticles

The agar-well diffusion experiment demonstrated the noteworthy antibacterial efficacy of CS-casein-Amla nanoparticles versus the examined clinical strains. The agar-well diffusion experiment demonstrated that adding 50 µl of CS-casein-Amla nanoparticles successfully suppressed the development of *P. aeruginosa*, as seen in Fig. 4. The antibacterial activity of CS-casein-Amla nanoparticles showed equal effectiveness versus all investigated isolates ($P<0.01$). Notably, the CS-casein-Amla nanoparticles exhibited the highest level of activity versus Strain2, Strain3, Strain6, Strain8, and Strain9, with a zone of inhibition of over 40 mm±0.62 ($P<0.0001$). The CS-casein-Amla nanoparticles exhibited the lowest level of activity versus Strain1, Strain4, Strain5, Strain7, and Strain10, with a zone of inhibition (mm) greater than 30 mm±0.62 ($P<0.001$).

Time kill assay

Figure 5 displays the growth profile and bacterial eradication achieved by CS-casein, Amla, and CS-casein-Amla nanoparticles at various amounts of each formulation. Each species has a different growth curve. *P. aeruginosa*

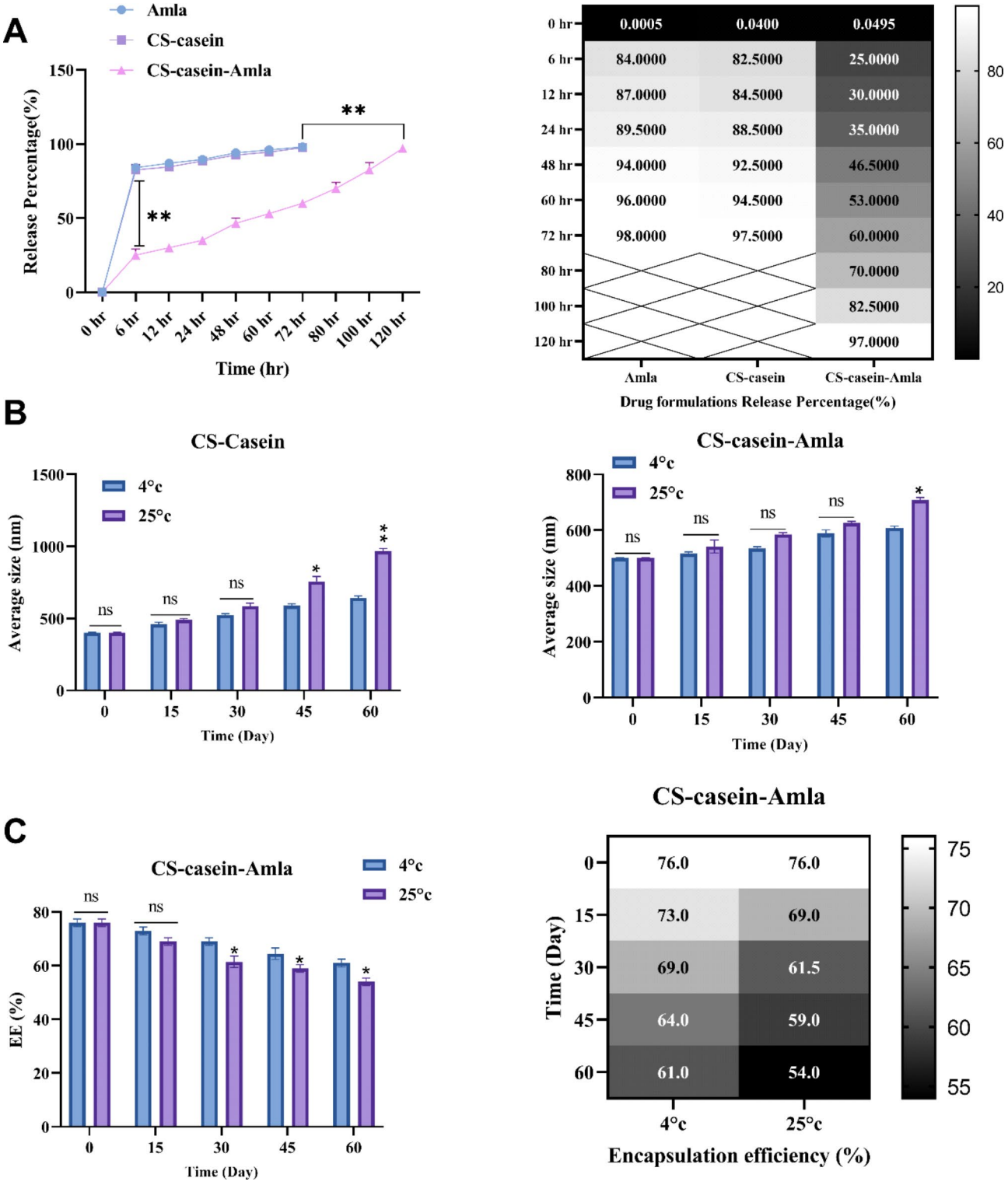

Fig. 3 (**A**) The regulated drug release of CS-casein and CS-casein-Amla is greater compared to Free Amla. (**B**) Investigating the impact of temperature on the average size of CS-casein and CS-casein-Amla. (**C**) The impact of temperature on the efficiency (EE%) of CS-casein-Amla nanoparticles

Table 6 MIC, SubMIC, MBC and MBIC value of free CS-casein, free Amla, and CS-casein-amla nanoparticles ($n=3$)

Sample	*P. aeruginosa*										
	Free CS-casein (µg/ml)				Free Amla (µg/ml)				CS-casein-Amla nanoparticles (µg/ml)			
	MBC	MIC	Sub-MIC	MBIC	MBC	MIC	Sub-MIC	MBIC	MBC	MIC	Sub-MIC	MBIC
Strain 1	---	---	---	---	100	50	25	12.5	6.25	3.125	1.56	0.781
Strain 2	100	50	25	25	50	25	12.5	12.5	3.125	1.56	0.781	0.781
Strain 3	100	50	25	25	50	25	12.5	12.5	3.125	1.56	0.781	0.781
Strain 4	100	50	25	25	100	50	25	12.5	6.25	3.125	1.56	0.781
Strain 5	100	50	25	25	100	50	25	12.5	6.25	3.125	1.56	0.781
Strain 6	100	50	25	25	50	25	12.5	12.5	3.125	1.56	0.781	0.781
Strain 7	---	---	---	---	100	50	25	12.5	6.25	3.125	1.56	0.781
Strain 8	100	50	25		50	25	12.5	12.5	3.125	1.56	0.781	0.781
Strain 9	100	50	25	25	50	25	12.5	12.5	3.125	1.56	0.781	0.781
Strain 10	---	---	---		100	50	25	12.5	6.25	3.125	1.56	0.781

Strains 2, 3, 5, 6, 8, and 9 had a lag phase of 4–8 h, and in every experiment, its maximal growth exceeded the growth of Strains 1, 4, 5, 7, and 10. The lag phase duration for *P. aeruginosa* Strain1, Strain4, Strain5, Strain7, and Strain10 was around 4 h. Overall, the bacterial population number of Strain1, Strain4, Strain5, Strain7, and Strain10 decreased less when exposed to CS-casein-Amla nanoparticles compared to Strain2, Strain3, Strain6, Strain8, and Strain9, as seen by the time-kill curves.

Anti-biofilm activity

P. aeruginosa strains were exposed to drug formulations for a short time, and the ability of free CS-casein and CS-casein-Amla nanoparticles to inhibit their growth by sticking to biofilm was compared to that of free Amla. Unlike the study of minimum biofilm inhibitory concentration (MBIC), the condition for inhibiting biofilm formation was more difficult. In this scenario, the biofilm was initially subjected to medication formulations or free Amla for merely two hours. Afterwards, the biofilms were rinsed and cultivated in a drug-free media for 24 h. The study used minimum inhibitory concentration (MIC) dosages for each strain. The concentration of the medication formulations was calculated based on the minimum inhibitory concentration (MIC) of free Amla. The findings were quantified as the percentage of inhibition of biofilm formation (BGI%) and shown in Fig. 6.

Biofilm gene transcription analysis

Quantitative Real-Time PCR was employed to investigate the transcription of *PpgL*, *BdlA*, *and GacA* biofilm genes utilizing subMIC dosages of Amla, CS-casein, and CS-casein-Amla. The findings indicate that the transcription of *PpgL*, *BdlA*, *and GacA* biofilm genes showed the most significant decrease following treatment with CS-casein-Amla ($p<0.01$) (Fig. 7). Furthermore, Amla exhibited a substantial decrease in the amount of transcription of biofilm genes when compared to CS-casein ($p<0.05$).

The findings demonstrate a substantial reduction in the mRNA levels of *PpgL*, *BdlA*, *and GacA* after administration with free Amla and CS-casein-Amla nanoparticles compared to the CS-casein group. These findings indicate that both free Amla and CS-casein-Amla nanoparticles have antibiofilm properties compared to *P. aeruginosa* strains.

Cytotoxicity

The cytotoxic properties of Amla, CS-casein, and CS-casein-Amla nanoparticles were assessed in PBS on the HDF normal cell line. The CS-casein-Amla nanoparticles exhibited little cytotoxicity compared to free Amla at all evaluated doses. Approximately 76±1.33% of the cells injected with Amla remained alive 24 h after exposure to the MIC concentration (50 µg/ml) treatment. In contrast,

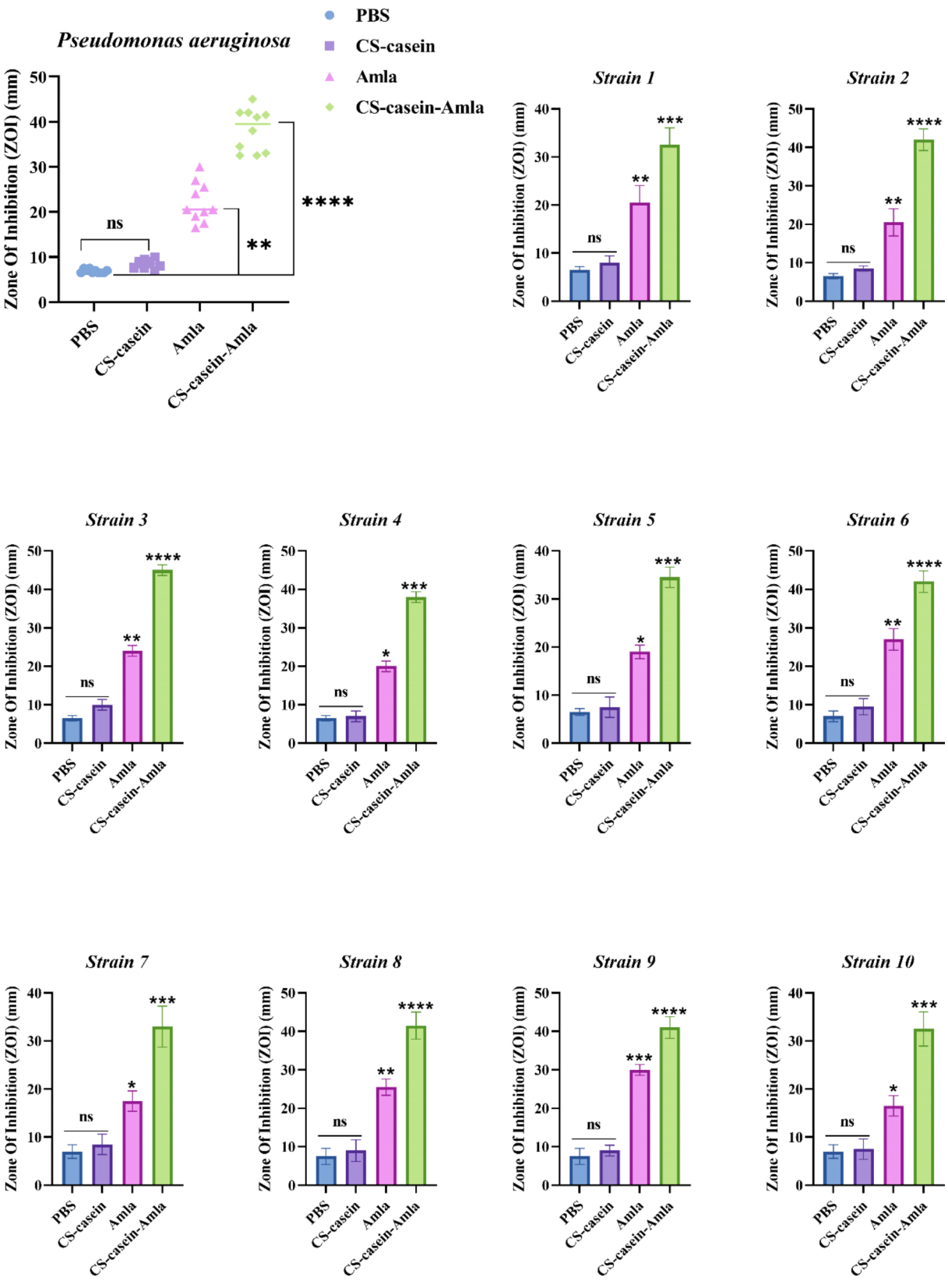

Fig. 4 Antibacterial activity PBS, Amla, CS-casein, and CS-casein-Amla nanoparticles against tested clinical isolates

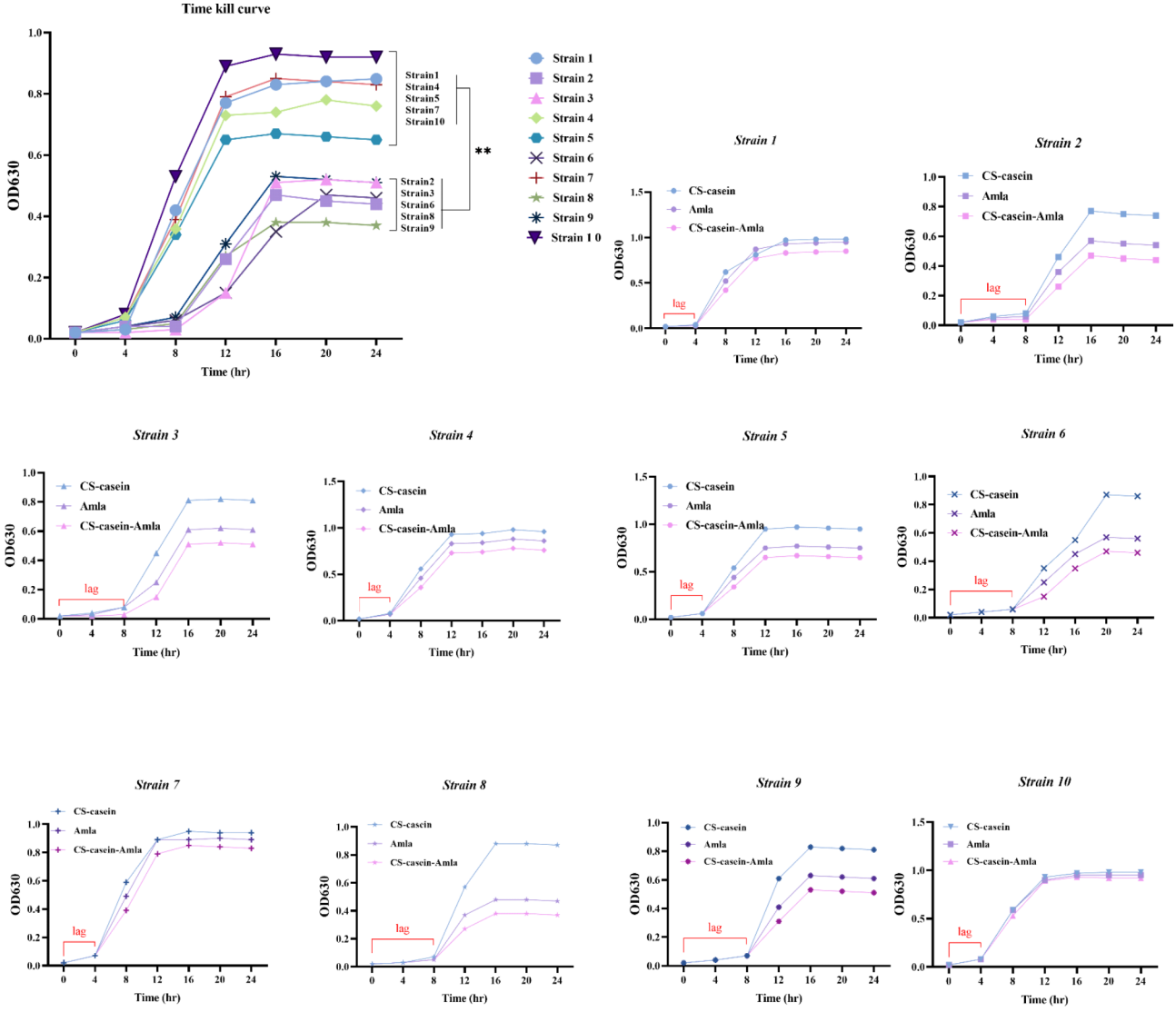

Fig. 5 Time–kill curves of CS-casein, Amla, and CS-casein-Amla nanoparticles against clinical Strains of *P. aeruginosa*

more than 90±1.37% of the cells remained alive 24 h after being incubated with the MIC concentration (3.125 µg/ml) of CS-casein-Amla nanoparticles. The cell survival rates after 72 h were determined to be 88.5±1.44%, 71±2.14%, and 88.7±2.18% for the MIC concentration of CS-casein, Amla, and CS-casein-Amla nanoparticles, respectively (Fig. 8). In contrast, the proportion of cells that survived 72 h after being treated with PBS was 93.7±2.71%. The flow chart of the synthesis steps of CS-casein and CS-casein-Amla nanoparticles was shown in Fig. 9.

Discussion

The desiccated fruits of amla are used in the Unani system of medicine for the management of haemorrhage, diarrhoea, and dysentery [30]. Amla is known to possess antiviral, antibacterial, antifungal, antihelminthic, and anti-inflammatory effects, as stated [31]. Several bioactive chemicals found in amla have been discovered, including flavonoids such as quercetin, ascorbic acid, gallic acid, alkaloids like phyllantine and phyllantidine, hydrolysable tannins such as emblicanin A and B, punigluconin, and pedunculagin. The presence of tannins in amla is responsible for its antioxidant action [30, 31]. This work aimed to quantitatively evaluate the antibacterial activity of amla fruit extracts against *P. aeruginosa*, according to its known medicinal and antimicrobial capabilities.

Chitosan (CS) is a crucial product of chitin obtained by eliminating the acetate component. Chitosan is derived from fungi's cell walls and crustaceans' exoskeletons, such as crabs and prawns [32]. In this study, we produced CS nanoparticles using the ionic gelation method by combining chitosan with tripolyphosphate

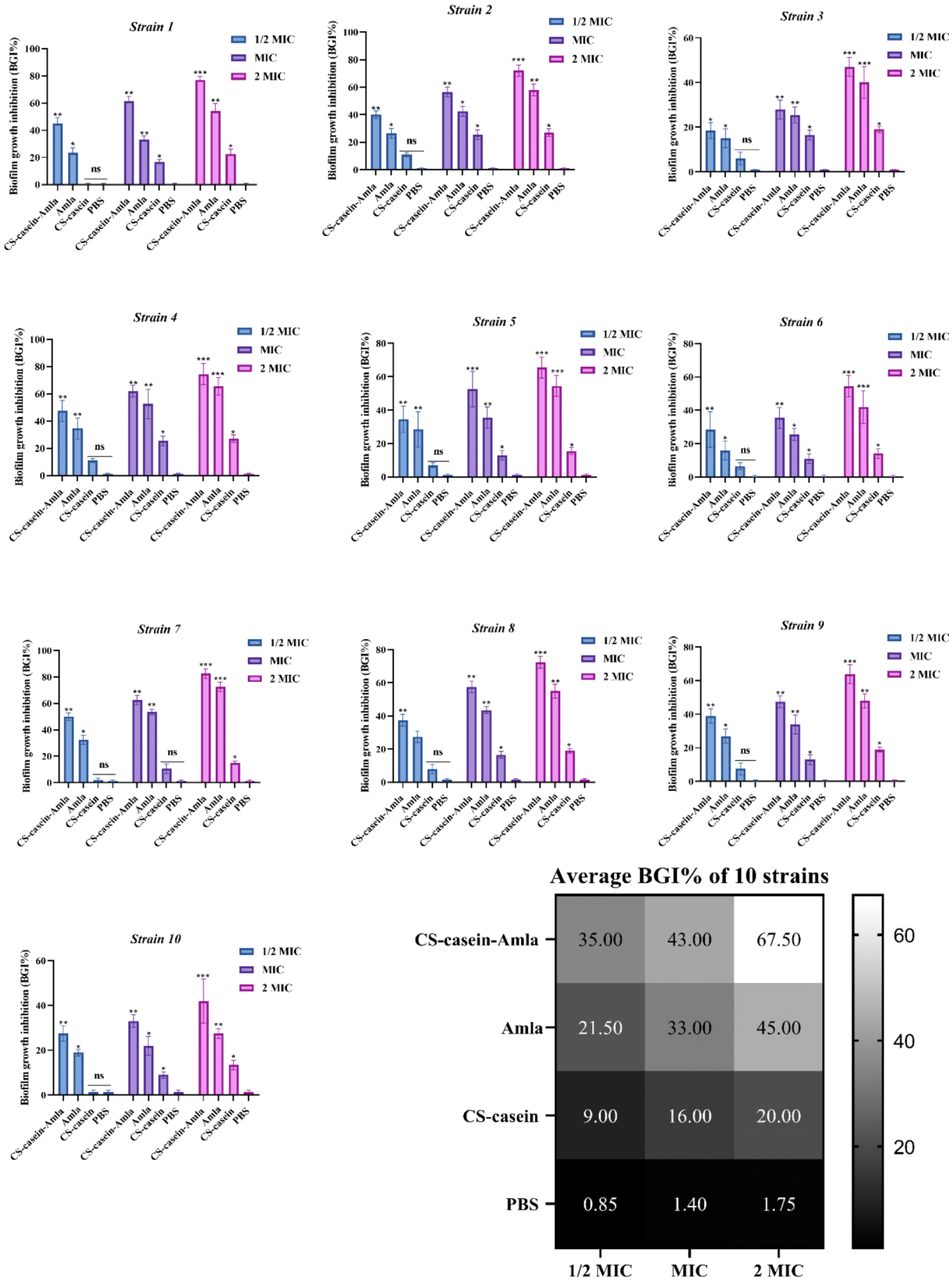

Fig. 6 The percentage of biofilm growth inhibition (BGI%) was measured for Amla, CS-casein, and CS-casein-Amla. The data shown are the mean value plus or minus the standard deviation (SD) of three separate and independent studies. The significance threshold was established as *** $p < 0.001$, ** $p < 0.01$, * $p < 0.05$

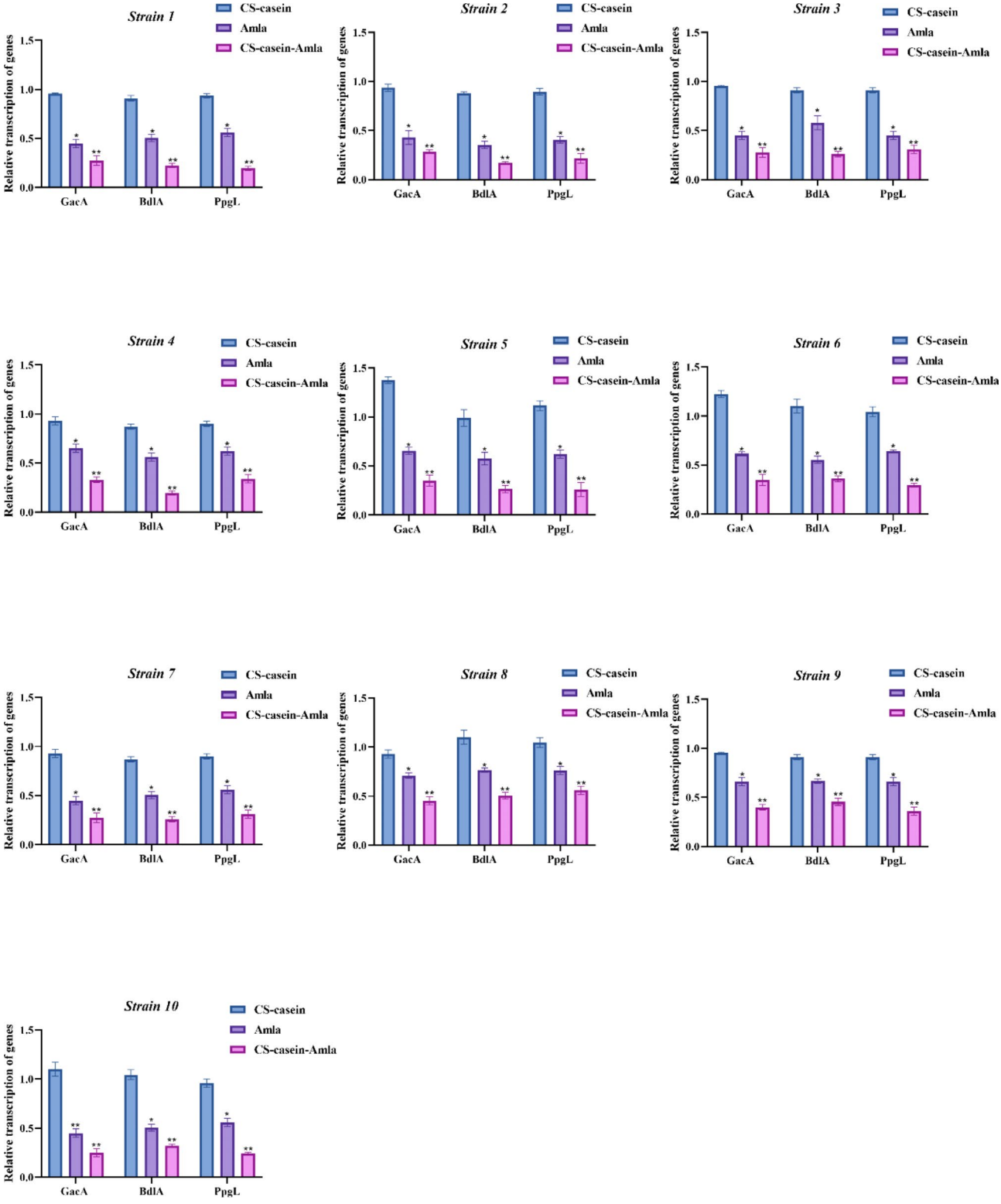

Fig. 7 The effect of Amla, CS-casein, and CS-casein-Amla nanoparticles on the transcription of *PpgL*, *BdlA*, *and GacA* biofilm genes. The data shown are the mean value ± standard deviation (SD) obtained from three separate and independent studies. The significance threshold was established as ** $p < 0.01$, * $p < 0.05$

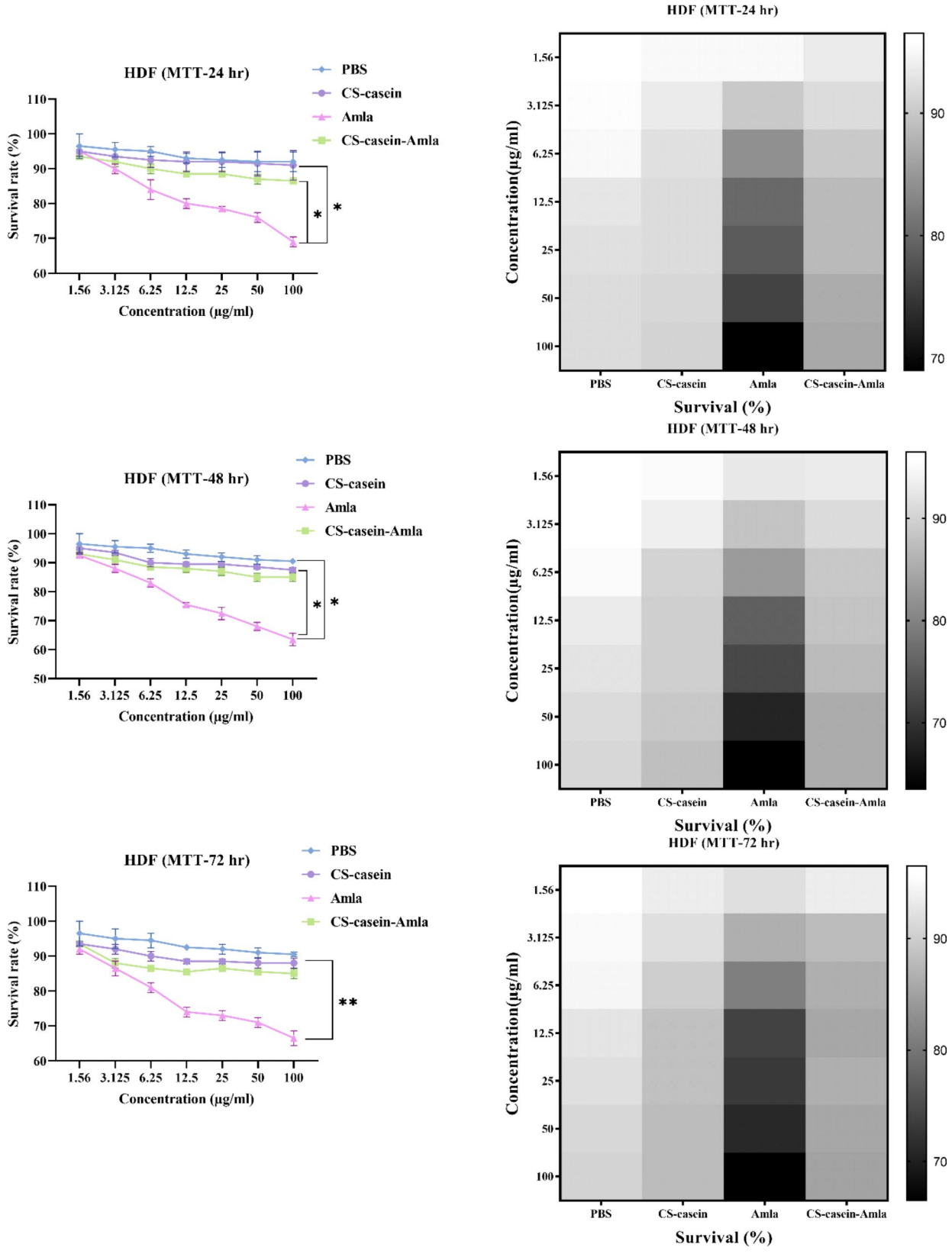

Fig. 8 The cell survival percentage of HDF cells administered by Amla, CS-casein, and CS-casein-Amla nanoparticles was compared to that of cells treated with PBS for 24, 48, and 72 h

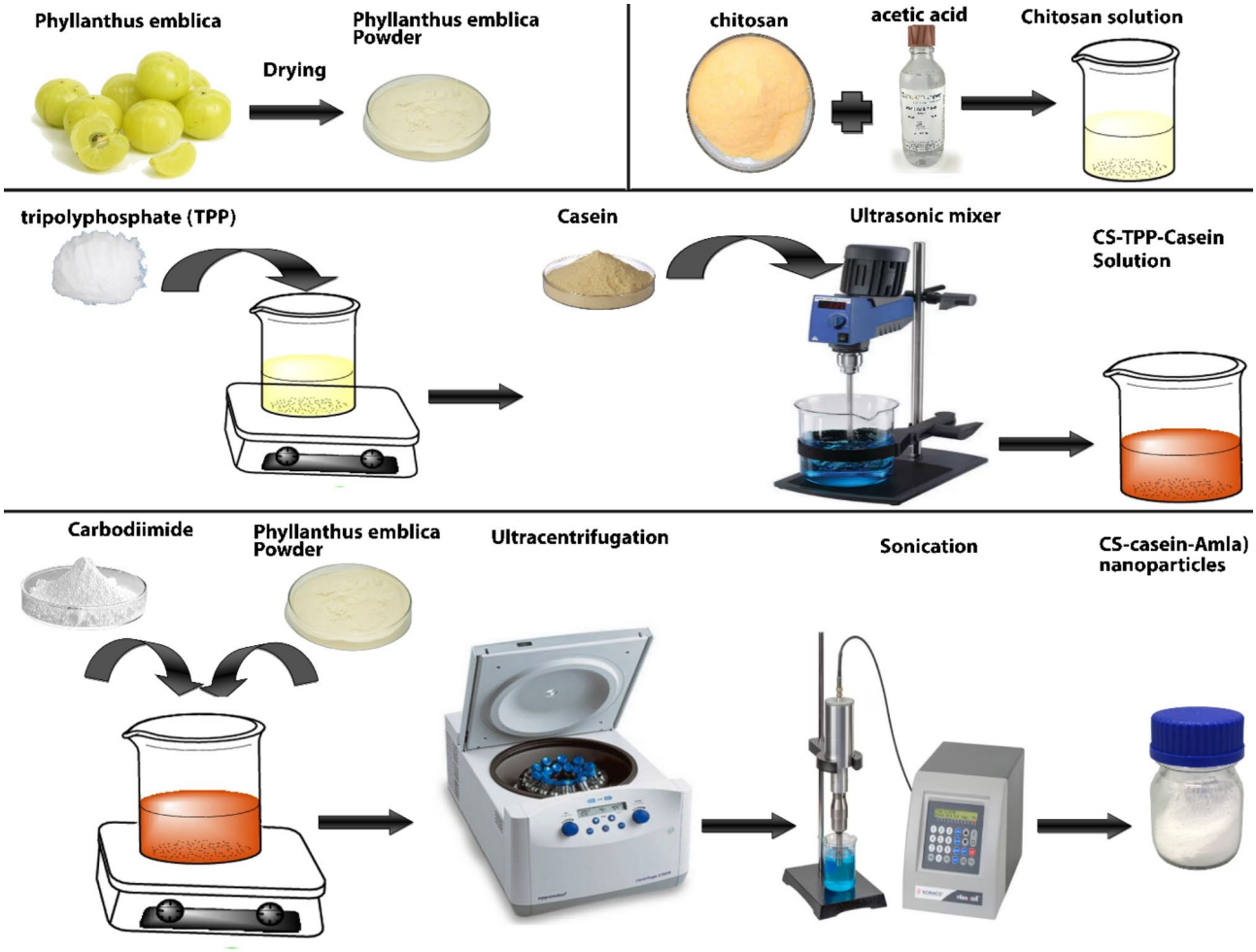

Fig. 9 Flowchart of the synthesis steps of CS-casein, and CS-casein-Amla nanoparticles

and casein anions. Understanding particle sizing might need to be clarified due to the various methodologies and accompanying instruments [33]. The size of CS-casein nanoparticles is significantly influenced by the production parameters, including the pH of the preparation medium and the amount of CS, TPP, and Amla. Within this particular context, the data presented here demonstrate that the freeze-drying procedure applied stress to the particles throughout the preparation, resulting in a noticeable particle size enlargement [34]. The notable disparity between the two measurements may be attributed to FeSEM observations capturing configurations in the dehydrated state. At the same time, those acquired using laser diffraction represent the hydrodynamic diameter. In addition, the areas of chitosan that are not covered with Amla undergo swelling, which can distort particle size determination.

The present study aimed to enhance the antibacterial efficacy of *P. aeruginosa* strains by using CS-casein-Amla nanoparticles. CS-casein-Amla nanoparticles were synthesized by combining negative-ionic casein with chitosan. To ensure consistency in the formulations and maintain a uniform surface load of Amla, the amount of casein was maintained consistently throughout all formulations. This was done since varying quantities of casein may lead to varied effects and actions in the formulations. Conversely, different combinations of peptides resulted in nanostructures exhibiting diverse morphological properties [35]. Varying outcomes were achieved when the proportions of casein and chitosan were equivalent. The disparity in ZP values may be ascribed to the decrease in the quantity of unbound amino groups on CS resulting from the grafting of casein. This indicates the creation of the CS-casein nanoparticles [21]. Nevertheless, some chitosan chains were present in surplus and had a role in maintaining the stability of the particles [36]. ART-FTIR verified the development of the CS-casein complex. The existence of $-NH3+$ in CS-casein was confirmed by the appearance of peaks associated explicitly with the absorption of $-NH3+$ in CS.

P. aeruginosa is a common hospital pathogen that has become more widespread worldwide in the last thirty

years. It presents a significant risk as a nosocomial infection. *P. aeruginosa* strains have a high resistance level to a broad spectrum of antimicrobial drugs, with some strains demonstrating multi-drug resistance [37]. The formation of biofilms in *P. aeruginosa* strains hinders the entry of antimicrobial drugs and adds complexity to treating illnesses caused by these bacteria [38]. The synthesis of exoenzymes and secondary metabolites in Pseudomonas species depends on the global activator GacA, an extremely conserved reaction regulator in Gram-negative bacteria. The BdlA protein has an MCP (methyl-accepting chemotaxis protein) region and two PAS (Per-Arnt-Sim) domains, which are critical for environmental signal response in other proteins. Periplasmic gluconolactonase PpgL has been implicated in the control of the quorum-sensing (QS) system in P. aeruginosa. These proteins collaborate to form biofilm and facilitate quorum sensing in Pseudomonas aeruginosa, hence enhancing its resistance to many drugs [38, 52]. Consequently, it is crucial to research novel treatment options and methods to reduce resistance in *P. aeruginosa*. The findings of *P. aeruginosa* biofilm development in a controlled environment are consistent with a recent study, which observed an elevated rate of biofilm formation in *P. aeruginosa* [39]. Our investigation revealed that *P. aeruginosa* strains had the capacity to generate biofilm with significant robustness. Recent research has shown that auto-regulatory molecules may affect the structure of biofilms, the response to stress, and the tolerance to polymyxins in *P. aeruginosa* [40].

The resistance of bacterial biofilms to antimicrobials is a crucial subject of study in several research programs that aim to explore alternate sources of biocompatible materials derived from live organisms. Prior research has shown the efficacy of chemically modified chitosan derivatives, which include N- and O-substitution, copolymerization, and grafting, in combating bacteria that form biofilms. Nevertheless, the fundamental mechanisms still need better understood [41]. Research has shown that incorporating lipophilic moieties into quaternary ammonium-modified chitosan greatly enhances the material's ability to prevent the formation of biofilms. The most potent antibiofilm agent against S. aureus was N-Acetyl-N-stearoyl-N′, N′′, N-trimethyl chitosan, a compound with two hydrophobic groups, namely acetyl and stearoyl [42]. N-acetyl-N-stearoyl-N′, N′′, N′′-trimethyl chitosan has a greater capacity to enter biofilms, resulting in a four-fold decrease in minimum biofilm eradication concentration (MBEC) compared to a control without lipophilic components [43].

Prior research has shown that ZnO nanoparticles had antibiofilm properties. This is because ZnO nanoparticles are characterized by their tiny size and large specific surface area, which results in their strong oxidation ability [44]. The findings of this investigation were similar to another study, which showed that chitosan-alginate (CS/ALG) microspheres effectively prevented the development of bacterial biofilms in S. aureus, E. faecalis, *P. aeruginosa*, and P. vulgaris following a single treatment with 40 µg. Chitosan may readily interact with the cell membrane of bacteria with a negative charge. This interaction can disrupt the permeability of the bacterial cell membrane and interfere with the function of membrane proteins, ultimately disrupting the structure and function of the bacteria [45]. Based on the results of this study, it can be shown that CS-casein nanoparticles effectively hinder the formation of the biofilm layer and demonstrate significant inhibitory properties. Chitosan nanoparticles, which included several forms of chitosan, such as low- and high-molecular-weight chitosan compounds, exhibited antibacterial properties that inhibited the establishment of bacterial biofilms.

The CS-casein-Amla nanoparticles, synthesized using chitosan, demonstrated strong antibacterial activity against gram-negative strains of *P. aeruginosa*. The positively charged composition of the chitosan improved the uptake into the negatively charged membranes of cells of harmful bacteria [46]. Undoubtedly, the CS-casein complex may shield chitosan from degradation by glycoside hydrolyzing enzymes such as chitinases or chitosanases synthesized by these bacteria [47]. The research demonstrated strong suppression of S. aureus and E. coli utilizing CS-nanoparticles in the presence of TPP [48–50]. Chitosan compounds with a significant amount of substitution and moderate molecular weight showed better antibacterial activity when compared to commercial antibiotics. Moreover, it was shown that chitosan with different molecular weights had improved antibacterial effectiveness when the degree of substitution was raised [47, 48]. Nevertheless, studies have shown that polymers like starch and starch-stabilized Ag nanoparticles have proven effective in fighting bacteria. These polymers can disrupt biofilm formation and eliminate intracellular mycobacteria at concentrations lethal to bacteria but do not harm mammalian macrophages. This was linked to the human cationic antibacterial peptide LL-37 [47, 48]. The inhibitory effect on bacterial growth is caused by the positively charged chitosan's capacity to break the bacteria's negatively charged cell membranes [48, 50–52]. It is important to note that comprehending the antibacterial process is difficult because of the differences in cell surface features between Gram-positive and Gram-negative bacteria.

Conclusion

Nanoparticles have developed as novel instruments that provide a viable alternative to antibiotics for directly or indirectly battling dangerous bacterial diseases. CS has

also been investigated as a medication carrier because of its biocompatible characteristics. This work aimed to create CS-casein-Amla nanoparticles by crosslinking casein onto the surface of CS-TPP particles. This nano-system exhibited exceptional antibiofilm activity and antibacterial efficacy against several strains of *P. aeruginosa*. These encouraging findings establish this innovative technology as a cost-effective, secure, and efficient approach to combat bacterial infections and a viable vehicle for delivering antibacterial medications to enhance their effectiveness. Given the novelty of employing nanoparticles, it is crucial to assess potential dangers carefully. In future studies, it is important to conduct in vitro experiments that examine the essential characteristics of CS-casein, including their bio-persistence and potential processes.

Supplementary Information

The online version contains supplementary material available at https://doi.org/10.1186/s12896-024-00907-9.

Supplementary Material 1

Acknowledgements
The authors would like to thank the staff members of the Biotechnology Research Center of the Islamic Azad University of Shahrekord Branch in Iran for their help and support. This research received no specific grant from public, commercial, or not-for-profit funding agencies.

Author contributions
Conceptualization, H.S., H.R.; methodology, H.S.; software, H.R. and L.R.; All authors reviewed the manuscript.

Funding
This research received no specific grant from funding agencies in the public, commercial, or not-for-profit sectors.

Data availability
The datasets analyzed during the current study are available from the corresponding author upon reasonable request.

Declarations

Ethics approval and consent
The study was approved by the Ethics Committee of the Islamic Azad University of Shahrekord Branch in Iran (IR.IAU.SHK.REC.1402).

Consent to publish
Not applicable.

Competing interests
The authors declare no competing interests.

Received: 30 August 2024 / Accepted: 4 October 2024
Published online: 18 December 2024

References

1. Karunamoorthi K, Jegajeevanram K, Vijayalakshmi J, Mengistie E. Traditional medicinal plants: a source of phytotherapeutic modality in resource-constrained health care settings. J Evidence-Based Complement Altern Med. 2013;18(1):67–74.
2. Piri Gharaghie T, Hajimohammadi S. C*Gac*Arison of anti-candida effects of aqueous, ethanolic extracts and essential oil of E. Angustifolia with fluconazole on the growth of clinical strains of Candida. New Cell Mol Biotechnol J. 2021;11(43):25–38.
3. Mal A, Meena DS. *Phyllanthus emblica*: a herbal remedy for healthy life. ECS Trans. 2022;107(1):3199.
4. Ahmad B, Hafeez N, Rauf A, Bashir S, Linfang H, Rehman MU, Mubarak MS, Uddin MS, Bawazeer S, Shariati MA, Daglia M. *Phyllanthus embaica*: A comprehensive review of its therapeutic benefits. South Afr J Bot. 2021;138:278–310.
5. Saini R, Sharma N, Oladeji OS, Sourirajan A, Dev K, Zengin G, El-Shazly M, Kumar V. Traditional uses, bioactive composition, pharmacology, and toxicology of *Phyllanthus emblica* fruits: a comprehensive review. J Ethnopharmacol. 2022;282:114570.
6. Piri Gharaghie T, Doosti A, Mirzaei SA. Prevalence and antibiotic resistance pattern of Acinetobacter spp. infections in Shahrekord medical centers. Dev Biol. 2021;13(4):35–46.
7. Ghajari G, Naser RH, Pecho RD, Alhili F, Piri-Gharaghie T. Chitosan/Pectin Nanoparticles Encapsulated with Echinacea pallida: a focus on Antibacterial and Antibiofilm Activity against Multidrug-Resistant Staphylococcus aureus. Appl Biochem Biotechnol. 2023 Sep;1:1–21.
8. Sharma G, Rao S, Bansal A, Dang S, Gupta S, Gabrani R. *P. aeruginosa* biofilm: potential therapeutic targets. Biologicals. 2014;42(1):1–7.
9. Despotovic A, Milosevic B, Milosevic I, Mitrovic N, Cirkovic A, Jovanovic S, Stevanovic G. Hospital-acquired infections in the adult intensive care unit—Epidemiology, antimicrobial resistance patterns, and risk factors for acquisition and mortality. Am J Infect Control. 2020;48(10):1211–5.
10. Yin R, Cheng J, Wang J, Li P, Lin J. Treatment of *P. Aeruginosa* infectious biofilms: challenges and strategies. Front Microbiol. 2022;13:955286.
11. Taghiloo S, Piri-Gharaghie T, Zand Z, Kabiri-Samani S, Kabiri H, Rajaei N. Echinacea angustifolia encapsulated with alginate/chitosan nanoparticles as a novel candidate carrier for combating multidrug-resistant Staphylococcus aureus. J Drug Deliv Sci Technol. 2021;67:28–32.
12. Deena SR, Kumar G, Vickram AS, Singhania RR, Dong CD, Rohini K, Anbarasu K, Thanigaivel S, Ponnusamy VK. Efficiency of various biofilm carriers and microbial interactions with substrate in moving bed-biofilm reactor for environmental wastewater treatment. Bioresour Technol. 2022;359:127421.
13. Bartoloni A, Gotuzzo E. Bacterial-resistant infections in resource-limited countries. Antimicrob Resist Developing Ctries. 2010:199–231.
14. Murugaiyan J, Kumar PA, Rao GS, Iskandar K, Hawser S, Hays JP, Mohsen Y, Adukkadukkam S, Awuah WA, Jose RA, Sylvia N. Progress in alternative strategies to combat antimicrobial resistance: focus on antibiotics. Antibiotics. 2022;11(2):200.
15. Asadipour E, Asgari M, Mousavi P, Piri-Gharaghie T, Ghajari G, Mirzaie A. Nanobiotechnology and challenges of drug delivery system in cancer treatment pathway. Chem Biodivers. 2023;20(6):e202201072.
16. Mangla B, Javed S, Sultan MH, Ahsan W, Aggarwal G, Kohli K. Nanocarriers-assisted needle-free vaccine delivery through oral and intranasal transmucosal routes: a novel therapeutic conduit. Front Pharmacol. 2022;12:757761.
17. Mikušová V, Mikuš P. Advances in chitosan-based nanoparticles for drug delivery. Int J Mol Sci. 2021;22(17):9652.
18. Mu H, Guo F, Niu H, Liu Q, Wang S, Duan J. Chitosan improves anti-biofilm efficacy of gentamicin through facilitating antibiotic penetration. Int J Mol Sci. 2014;15(12):22296–308.
19. Mu H, Zhang A, Zhang L, Niu H, Duan J. Inhibitory effects of chitosan in combination with antibiotics on Listeria monocytogenes biofilm. Food Control. 2014;38:215–20.
20. Siddhardha B, Pandey U, Kaviyarasu K, Pala R, Syed A, Bahkali AH, Elgorban AM. Chrysin-loaded chitosan nanoparticles potentiates antibiofilm activity against Staphylococcus aureus. Pathogens. 2020;9(2):115.
21. Alshweiat A, Al-Khresieh RO, Alzarieni KZ, Rashaid AH. A significant antibiofilm and antimicrobial activity of chitosan-polyacrylic acid nanoparticles against pathogenic bacteria. Saudi Pharm J. 2024;32(1):101918.
22. Rashki S, Safardoust-Hojaghan H, Mirzaei H, Abdulsahib WK, Mahdi MA, Salavati-Niasari M, Khaledi A, Khorshidi A, Mousavi SG. Delivery LL37 by chitosan nanoparticles for enhanced antibacterial and antibiofilm efficacy. Carbohydr Polym. 2022;291:119634.
23. Ramos J, Forcada J, Hidalgo-Alvarez R. Cationic polymer nanoparticles and nanogels: from synthesis to biotechnological applications. Chem Rev. 2014;114(1):367–428.
24. Sadiq U, Gill H, Chandrapala J. Casein micelles as an emerging delivery system for bioactive food components. Foods. 2021;10(8):1965.
25. Głąb TK, Boratyński J. Potential of casein as a carrier for biologically active agents. Top Curr Chem. 2017;375:1–20.

26. Xu J, Lin Q, Sheng M, Ding T, Li B, Gao Y, Tan Y. Antibiofilm effect of cinnamaldehyde-chitosan nanoparticles against the biofilm of Staphylococcus aureus. Antibiotics. 2022;11(10):1403.
27. Elzoghby AO, El-Fotoh WS, Elgindy NA. Casein-based formulations as promising controlled release drug delivery systems. J Controlled Release. 2011;153(3):206–16.
28. Zhang F, Cai X, Ding L, Wang S. Effect of pH, ionic strength, chitosan deacetylation on the stability and rheological properties of O/W emulsions formulated with chitosan/casein complexes. Food Hydrocolloids. 2021;111:106211.
29. Liang LI, Luo Y. Casein and pectin: structures, interactions, and applications. Trends Food Sci Technol. 2020;97:391–403.
30. Jamali MC. Antimicrobial activity of *Phyllanthus emblica*. J Bio Innov. 2016;5(6):979–84.
31. Khurana SK, Tiwari R, Sharun K. Mohd. Iqbal Yatoo, Mudasir Bashir Gugjoo and Kuldeep Dhama, Emblica officinalis (Amla) with a Particular Focus on its antimicrobial potentials: a review. J Pure Appl Microbiol. 2019;13(4):1995–2012.
32. Santos VP, Marques NS, Maia PC, Lima MA, Franco LD, Campos-Takaki GM. Seafood waste as attractive source of chitin and chitosan production and their applications. Int J Mol Sci. 2020;21(12):4290.
33. Shekunov BY, Chattopadhyay P, Tong HH, Chow AH. Particle size analysis in pharmaceutics: principles, methods and applications. Pharm Res. 2007;24:203–27.
34. Oyinloye TM, Yoon WB. Effect of freeze-drying on quality and grinding process of food produce: a review. Processes. 2020;8(3):354.
35. Khatun S, Appidi T, Rengan AK. Casein nanoformulations-potential biomaterials in theranostics. Food Bioscience. 2022;50:102200.
36. Klinkesorn U. The role of chitosan in emulsion formation and stabilization. Food Reviews Int. 2013;29(4):371–93.
37. Botelho J, Grosso F, Peixe L. Antibiotic resistance in *P. aeruginosa*–Mechanisms, epidemiology and evolution. Drug Resist Updates. 2019;44:100640.
38. Qin S, Xiao W, Zhou C, Pu Q, Deng X, Lan L, Liang H, Song X, Wu M. *P. aeruginosa*: pathogenesis, virulence factors, antibiotic resistance, interaction with host, technology advances and emerging therapeutics. Signal Transduct Target Therapy. 2022;7(1):199.
39. de Sousa T, Hébraud M, Alves O, Costa E, Maltez L, Pereira JE, Martins Â, Igrejas G, Poeta P. Study of antimicrobial resistance, biofilm formation, and motility of *P. Aeruginosa* derived from urine samples. Microorganisms. 2023;11(5):1345.
40. Chevalier S, Bouffartigues E, Bazire A, Tahrioui A, Duchesne R, Tortuel D, Maillot O, Clamens T, Orange N, Feuilloley MG, Lesouhaitier O. Extracytoplasmic function sigma factors in P. Aeruginosa. Biochim et Biophys Acta (BBA)-Gene Regul Mech. 2019;1862(7):706–21.
41. Yan D, Li Y, Liu Y, Li N, Zhang X, Yan C. Antimicrobial properties of chitosan and chitosan derivatives in the treatment of enteric infections. Molecules. 2021;26(23):7136.
42. Sahariah P, Másson M, Meyer RL. Quaternary ammoniumyl chitosan derivatives for eradication of staphylococcus aureus biofilms. Biomacromolecules. 2018;19(9):3649–58.
43. Si Z, Zheng W, Prananty D, Li J, Koh CH, Kang ET, Pethe K, Chan-Park MB. Polymers as advanced antibacterial and antibiofilm agents for direct and combination therapies. Chem Sci. 2022;13(2):345–64.
44. Alves MM, Bouchami O, Tavares A, Cordoba L, Santos CF, Miragaia M, de Fátima Montemor M. New insights into antibiofilm effect of a nanosized ZnO coating against the pathogenic methicillin resistant Staphylococcus aureus. ACS Appl Mater Interfaces. 2017;9(34):28157–67.
45. Thaya R, Vaseeharan B, Sivakamavalli J, Iswarya A, Govindarajan M, Alharbi NS, Kadaikunnan S, Al-Anbr MN, Khaled JM, Benelli G. Synthesis of chitosan-alginate microspheres with high antimicrobial and antibiofilm activity against multi-drug resistant microbial pathogens. Microb Pathog. 2018;114:17–24.
46. Liu X, Xia W, Jiang Q, Xu Y, Yu P. Effect of kojic acid-grafted-chitosan oligosaccharides as a novel antibacterial agent on cell membrane of gram-positive and gram-negative bacteria. J Biosci Bioeng. 2015;120(3):335–9.
47. Kritchenkov AS, Egorov AR, Artemjev AA, Kritchenkov IS, Volkova OV, Kurliuk AV, Shakola TV, Rubanik VV Jr, Rubanik VV, Tskhovrebov AG, Yagafarov NZ. Ultrasound-assisted catalyst-free thiol-yne click reaction in Chitosan chemistry: Antibacterial and transfection activity of novel cationic chitosan derivatives and their based nanoparticles. Int J Biol Macromol. 2020;143:143–52.
48. Mohanty S, Mishra S, Jena P, Jacob B, Sarkar B, Sonawane A. An investigation on the antibacterial, cytotoxic, and antibiofilm efficacy of starch-stabilized silver nanoparticles. Nanomed Nanotechnol Biol Med. 2012;8(6):916–24.
49. Kharlamova A, Nicolai T, Chassenieux C. Heat-induced gelation of mixtures of casein micelles with whey protein aggregates. Food Hydrocolloids. 2019;92:198–207.
50. Morilla MJ, Ghosal K, Romero EL. Nanomedicines against Chagas disease: a critical review. Beilstein J Nanotechnol. 2024;15(1):333–49.
51. Jerez HE, Simioni YR, Ghosal K, Morilla MJ, Romero EL. Cholesterol nanoarchaeosomes for alendronate targeted delivery as an anti-endothelial dysfunction agent. Beilstein J Nanotechnol. 2024;15(1):517–34.
52. Song YJ, Wang KL, Shen YL, Gao J, Li T, Zhu YB, Li CC, He LH, Zhou QX, Zhao NL, Zhao C. Structural and functional insights into PpgL, a metal-independent β-propeller gluconolactonase that contributes to Pseudomonas aeruginosa virulence. Infect Immun. 2019;87(4):10–128.

Publisher's note